

Cerebrospinal fluid circulating tumor DNA depicts profiling of brain metastasis in NSCLC

Longbo Zhang (✉ longbo.zhang@yale.edu)

Yale School of Medicine <https://orcid.org/0000-0002-9077-3239>

Jun Wu

Central South University

Zhiqiang Liu

Erasmus University Rotterdam

Tianxiang Huang

Central South University

Ying Wang

Central South University

Mengmeng Song

Geneplus-Beijing Institute

Tao Song

Central South University

Xiaobing Zhang

Florida State University

Xi Li

Central South University

Gretchen Long

Yale School of Medicine

Article

Keywords:

Posted Date: April 26th, 2022

DOI: <https://doi.org/10.21203/rs.3.rs-1509960/v1>

License: © ⓘ This work is licensed under a Creative Commons Attribution 4.0 International License.

[Read Full License](#)

Abstract

Brain metastasis (BM) genetically diverges from the primary tumor in non-small-cell lung cancer (NSCLC). Hence, accurately capturing clinically relevant alterations is pivotal for the delivery of targeted therapies. Circulating tumor DNA (ctDNA) sequencing has emerged as a promising liquid biopsy in the biomarker-based clinical management of recurrent and extracranial metastatic NSCLC. However, absence of simultaneous sequencing data from brain metastatic sites prevents the definitive evaluation of the efficacy of ctDNA representing genetic profiles in BM. Here, we performed parallel genomic comparisons between matched BM and primary tumor DNA, plasma ctDNA, and cerebrospinal fluid (CSF) ctDNA. The results indicated that CSF ctDNA had a greater ability than plasma ctDNA in comprehensively representing the mutational landscape of BM, with CSF ctDNA detecting all BM mutations in 83.33% of patients while plasma ctDNA was only 27.78%. Mutant allele frequency (MAF) in CSF ctDNA was highly correlated with the tumor size of BM ($r = 0.95$), and the mean MAF in CSF ctDNA was more abundant than that in plasma ctDNA (38.05% vs. 4.57%). MAF and tumor mutational burden (TMB) in CSF ctDNA were strongly associated with those in BM ($r = 0.96$ and 0.97 , respectively). Of note, CSF ctDNA had significantly higher concordance with BM than plasma ctDNA (99.33% vs. 67.44%), facilitating the identification of clinically relevant mutations. Moreover, we found that plasma ctDNA has stronger profiling performance with a concordance of 93.01% in multiple brain metastases, equivalent to CSF ctDNA. Collectively, our study indicates that CSF ctDNA is superior to plasma ctDNA in accurately represent the profiling of single BM, plasma ctDNA could be an alternative liquid biopsy material to be applied in multiple brain metastatic NSCLC.

Introduction

Lung cancer is the leading cause of cancer-related mortality worldwide. Non-small-cell lung cancer (NSCLC) constitutes 85% of cases of lung cancer, and up to 50% of NSCLC patients will eventually develop brain metastasis (BM)^{1,2}. Recently, biomarker-guided therapies, enabled by the rapid development of genomic technologies, have inspired targeted anticancer treatments that have shown to dramatically improve NSCLC patient outcomes³⁻⁸. However, the prognoses of the patients with BM remain poor. Brain metastatic sites are highly divergent from primary tumors and extracranial metastases although with a common ancestor shared⁹⁻¹¹. Hence, accurately identifying potential actionable mutations along with the discovery of acquired resistance mechanisms in real time would tremendously benefit clinical management of NSCLC patients with BM. However, given the challenge of tumor accessibility, it is urgent to establish a minimally invasive biopsy for comprehensively depicting gene abnormalities in BM.

Circulating tumor DNA (ctDNA) has emerged as a promising liquid biopsy in the diagnosis, characterization, and management of metastatic and recurrent cancers by an increasing body of clinical evidence across multiple cancer types¹². During the last decade, extensive efforts involving the measurement and analysis of ctDNA have promoted its transition from laboratory investigation to clinical

application¹³⁻¹⁵. In lung cancer management, plasma-derived ctDNA provides a minimally invasive sampling method for real-time assessment and rapid evaluation at the time of each clinical decision. Beyond identifying therapeutically actionable tumor alterations, dynamic monitoring of ctDNA burden during surveillance serves as an early predictor of response or non-response to therapies^{12,14,16-22}. Furthermore, ctDNA offers greater potential than conventional biopsy to timely characterize acquired drug resistance since it does not require surgical resection, enables dynamic measurement and early detection ahead of clinical or radiographic metastasis or relapse²³.

Although ctDNA is a rising star for guiding clinical management in patients with malignancies, some uncertainties remain. The performance of liquid biopsies versus that of simultaneous tumor biopsies has not been studied extensively¹². Few such studies so far have indicated that plasma ctDNA measurement generally fails to detect ~ 20% of alterations present in the tumor and presumably has an even greater failure in brain tumors²⁴⁻²⁶. The blood-brain barrier (BBB) is a major anatomical barrier that may limit the performance of ctDNA detection in plasma since it likely prevents tumor ctDNA in the central nervous system (CNS) from reaching the peripheral circulation system. Recent findings also show that high BBB permeability increases the levels of plasma ctDNA²⁷. Given the direct contact with the brain and relative ease of access, cerebrospinal fluid (CSF) could have major advantages over plasma for evaluating ctDNA for patients with primary and metastatic brain tumors. Of great clinical significance, several studies have demonstrated that analyzing CSF ctDNA offers a more sensitive and specific source of tumor-specific mutations compared to plasma ctDNA in primary brain tumors^{10,28}. Furthermore, CSF ctDNA has been recently suggested to be a potentially better option than plasma ctDNA for predicting genomic alterations in leptomeningeal metastasis in NSCLC patients by comparing primary lung cancer, CSF and plasma ctDNA^{29,30}. However, these pioneering studies are limited by the absence of sequencing data from metastatic sites which prevents the definitive evaluation. To fully explore the efficacy of CSF ctDNA representing genetic profiles in BM versus that of plasma ctDNA in our study, we compared the matched quartet (primary lung cancer, BM, plasma ctDNA, and CSF ctDNA) from the same brain metastatic NSCLC patients.

Our data showed that CSF ctDNA detected all BM mutations in 83.33% of brain metastatic NSCLC patients, where only 27.78% in plasma ctDNA. CSF ctDNA was strongly correlated with BM in mutant allele frequency (MAF, $r = 0.96$) as well as tumor mutational burden (TMB, $r = 0.97$). In addition, the mean MAF in CSF ctDNA was significantly higher than that in plasma ctDNA (38.05% vs. 4.57%), suggesting CSF ctDNA offers greater potential to detect genomic alterations in BM due to the limit of detection of the current ctDNA platform. Importantly, CSF ctDNA had significantly higher concordance with BM compared with plasma ctDNA (99.33% vs. 67.44%). A set of clinically relevant BM mutations were absent in plasma ctDNA and solely detected in CSF ctDNA, including *EGFR*, *KRAS*, *RET*, and *CDK13*. Of clinical interest, we found plasma ctDNA had comparable concordance (93.01%) to that of CSF ctDNA to recapitulate mutations only in the cases of multiple brain metastases. Together, our study indicates that CSF ctDNA has greater sensitivity as a high-quality diagnostic material over plasma ctDNA to depict the

comprehensive genomic alterations in BM, and when managing multiple brain metastatic NSCLC, plasma can serve as an alternative material for ctDNA-based biopsy.

Results

Patient characteristics

We retrospectively profiled 63 samples (primary lung tumor, brain metastasis, peripheral blood, and cerebrospinal fluid) from 20 newly diagnosed, untreated, histologically confirmed brain metastatic lung adenocarcinoma (LUAD) patients. Of the 20 patients, 15 had a single brain metastasis, whereas the rest of 5 cases developed multiple brain metastases (median: 3, range 2 ~ 4) diagnosed radiographically (Suppl. Figure 1A-B). In addition, 2 patients had extracranial metastases (liver and thyroid). Demographic and clinical characteristics of the 20-patient case series are listed in Suppl. Table 1. The mean sequencing depth of 20 brain metastases and 13 primary lung tumors were 987.65x and 856.15x, respectively (7 primary lung tumors had low-abundance DNA extraction through biopsy samples or surgical resections had been done in other hospitals). Target sequencing for ctDNA was successfully performed in 19 (95.00%) plasma samples and 11 (55.00%) CSF samples. With a function sequencing depth filtering, 18 plasma ctDNA (mean depth: 1878.89x) and 6 CSF ctDNA data (mean depth: 1643.50x) were proceeded to further analysis.

Genetic Divergence Of Brain Metastases And Primary Tumors

Previous studies have demonstrated that BM and their matched primary tumors are clonally related, yet genetically diverse. Each site harbors its own subset of unique mutations³¹. To confirm this divergence in our cohort, we performed a targeted sequencing on primary lung cancer and matched BM. The mean somatic TMB was 9.92 mutations per megabase (Mb) of DNA in primary lung cancer (range: 3 ~ 26, median: 5) and 9.35 mutations per Mb in BM (range: 2 ~ 27, median: 7.5; Suppl. Figure 2A-B). The top 20 statistically significant mutated genes in BM profiling were highlighted as well as patient characteristics including sex, number, regions of metastatic lesions and Ki67 index (Fig. 1A, mutational landscape of primary lung cancer shown in Suppl. Figure 3). Genetically, BM and primary lung tumor harbored somatic mutations majorly in *TP53* (75.00% BM, 69.23% lung), *EGFR* (30.00% BM, 46.15% lung) and *KRAS* (25.00% BM, 15.38% lung), and BM diverged from primary lung cancer with more frequent alterations in *MLL3*, *ATRX* and *RB1* (Fig. 1B). Several significant co-occurring alterations: *EPHA5* (*ARID1A*), *ATM* (*STK11*), *PIK3CG* (*INPP4B*), *ARID1A* (*LRP1B*) and *EPHA5* (*LRP1B*) were identified in BM (Suppl. Figure 2C). In addition, our data showed that the mean MAF was positively associated with Ki67 expression in BM, independent of tumor size (Fig. 1C, Suppl. Figure 2D). To further evaluate the genetic relevancy and divergence between primary lung cancer and BM, we analyzed the shared and independently evolved mutations in each individual. Results demonstrated that 61.53% (8 out of 13) of patients harbored alterations specifically in the BM that were not detected in matched primary cancer

(Fig. 1D). The MAFs in BM and primary lung cancer were correlated (Pearson $r = 0.54$, $P \ll 0.0001$; Fig. 1E), however, the mean MAF in BM was significantly higher than that in primary cancer (36.24% vs. 27.11%, $P \ll 0.0001$; Fig. 1F). Furthermore, we found that an average of 23.65% (95% confidence interval [CI], 0%-50%; Fig. 1G) somatic alterations in BM were not detected in primary lung cancer, including approved actionable mutations such as *EGFR*, molecularly targeted mutations in development such as *ERBB4*, and common tumor suppressor gene abnormalities such as *TP53* and *RB1*. Together, these genetic divergences indicate that profiling primary lung cancer is not sufficient to predict the mutations in BM. However, the accessibility of BM is challenging due to the region and number of brain lesions, the patient's physical status, and the willingness to undergo another invasive sampling. Hence, it is urgent to develop a minimally invasive biopsy procedure to accurately profile BM and identify actionable mutations to assist in targeted drug selection.

Plasma Ctdna Is Insufficient To Recapitulate Mutations In Brain Metastases

CtDNA-based liquid assays from the plasma of peripheral blood samples have demonstrated high concordance of genomic profiles compared to tissue-based sequencing within and across cancer types^{13,14}. To test the capability of plasma ctDNA in representing gene alterations in BM, we compared plasma ctDNA with matched BM. The data showed that only 27.78% of plasma ctDNA samples (5 out of 18) were successful in detecting all the mutations harbored in matched BM. The unidentified BM mutations by plasma ctDNA was 28.66% (Fig. 2A-B) including actionable gene alterations such as *EGFR*, *KRAS* and *RET*, tumor suppressor gene mutations *TP53* and *RB1*, investigational targeted mutations *ERBB4*, *HGF*, and potential biomarker *INPP4B* for guiding immune checkpoint inhibitors³². Pathway analysis revealed that the undetected mutations were enriched mainly in metabolic related processes, as well as cell cycle processes (Fig. 2C). Although MAF in plasma ctDNA is weakly correlated with that in BM (Pearson $r = 0.39$, $P \ll 0.0001$), the mean MAF in plasma ctDNA is significantly lower compared with that in BM (4.57% vs. 35.16%, $P \ll 0.0001$) except in patients with extracranial metastases (BM-LUAD 6 and 11, liver and thyroid metastases, respectively; Fig. 2D, Suppl. Figure 4B-C), which is in line with previous findings where extrathoracic metastasis has a higher MAF detected than no extrathoracic metastasis in NSCLC²⁵. We next analyzed the concordance by calculating the percentage of identified BM mutations also found in plasma ctDNA. The data indicated an average of 67.44% (95% CI: 33.33%-100%) concordance between BM and plasma ctDNA (Fig. 2E). Of note, plasma ctDNA had significant higher concordance with BM in the patients with multiple metastatic lesions (93.01% vs. 50.90% in single metastasis, $P = 0.0449$), regardless of sex, TMB, metastatic regions, tumor size, distance to ventricles or peritumor edema size (Fig. 2F, Suppl. Figure 4D-E, Suppl. Table 2), suggesting the number of metastatic lesions is the key factor to determine the concordance between BM and plasma ctDNA.

Csf Ctdna Analysis Is Representative Of Brain Metastatic Lesion

CSF is a potential alternative to obtain brain tumor ctDNA for analyzing mutations in BM given its direct contact with the brain. CtDNA in CSF is relatively concentrated since the blood-brain barrier prevents its cycling with the peripheral circulation system^{10,33}. To assess whether the genomic landscape of CSF ctDNA represents mutational profiling in BM, we sequenced the CSF ctDNA obtained from lumbar puncture before brain tumor resection. We found that 83.33% (5 out of 6) CSF ctDNA samples recapitulated all the mutations in matched BM (Suppl. Figure 5A; 1 out of 25 BM alterations was absent in CSF ctDNA sequencing in BM-LUAD 7). Overall, CSF ctDNA could identify 98.31% mutations harbored in BM with only 1.69% mutations undetected (Fig. 3A-B). The mean MAF in CSF ctDNA is equivalent to that in BM (39.93% vs. 39.58%) and significantly correlated with the size of metastatic lesion by MRI volumetric analyses (Pearson $r=0.95$, $P=0.0039$; Fig. 3C-D). In addition, MAF in CSF ctDNA was highly correlated with that in BM (Pearson $r=0.96$, $P=0.0001$; Fig. 3E), as well as TMB (Pearson $r=0.97$, $P=0.0003$; Suppl. Figure 5B-C). To further investigate whether CSF ctDNA profiling is sufficient to represent the alterations in BM, we analyzed the concordance between BM and CSF ctDNA. The result indicated that CSF ctDNA had an average of 99.33% (95% CI: 96%-100%) concordance with BM, which was significantly greater than that of plasma ctDNA (67.44%, $P=0.0125$; Fig. 3F). Altogether, these results suggest that CSF ctDNA may prove a more accurate at profiling BM than plasma ctDNA.

CSF ctDNA has a greater capacity to detect BM mutations than plasma ctDNA for single BM

To further assess whether CSF ctDNA is better than plasma ctDNA in comprehensively representing the mutational landscape of BM, we performed a clonal analysis that showed CSF ctDNA had a higher detection rate of clonal mutations than plasma ctDNA (100% vs. 72.73%; Suppl. Figure 6). Comparing the proportion of the shared mutations between BM and plasma ctDNA or CSF ctDNA demonstrated that CSF ctDNA had a significantly higher percentage of shared mutations with BM than plasma ctDNA (mean: 83.61% vs. 54.55%, $P=0.0098$; Fig. 4A). We then performed parallel analyses for matched trios (BM, plasma ctDNA, and CSF ctDNA) from 5 patients. The data showed that sampling of brain metastatic lesions detected a total of 52 somatic mutations with 51 identified in CSF ctDNA while only 39 were found in plasma ctDNA (Fisher exact test: $P=0.0009$; Fig. 4B). CSF ctDNA had equivalent MAF to BM, which was more abundant than plasma ctDNA (Fig. 4C). MAF in CSF ctDNA was highly correlated with that in BM compared with plasma ctDNA (Pearson $r=0.98$, $P=0.0001$ vs. 0.52, $P=0.0008$; Fig. 4D). Moreover, TMB in CSF ctDNA was significantly correlated with that in BM whereas plasma ctDNA was not (Pearson $r=0.99$, $P=0.0022$; Fig. 4E). CSF ctDNA had a higher percentage of shared mutations with BM compared with plasma ctDNA in all 5 patients (mean indicated by dotted line: 82.83% vs. 52.06%; Fig. 4F-G). Of interest, concordance analyses revealed that plasma ctDNA had a better performance of representing BM alterations in the patients with multiple metastases than those with single metastasis (Fig. 2F). Therefore, we asked whether multiple brain metastases could be an exceptional condition where plasma ctDNA is comparable to CSF ctDNA to depict BM mutations. The concordance result indicated

that plasma ctDNA had a similar power as CSF ctDNA to represent alterations in BM in the patients with multiple brain metastases (mean, 93.01% vs. 99.33%; Fig. 4H). Together, these data suggest that CSF ctDNA has an advantage in detecting mutations in BM superior to plasma ctDNA, and plasma ctDNA could be an alternative liquid biopsy material only in multiple brain metastatic NSCLC.

Csf Ctdna Facilitates The Targeted Treatment Of Brain Metastasis

Identification of actionable mutations in BM is essential for the selection and delivery of targeted therapies to promote favorable outcomes. By comparing profiling results from BM, plasma ctDNA, and CSF ctDNA (diagram: Fig. 5A), we found that CSF ctDNA had a better ability to detect clinically relevant alterations. In BM-LUAD 7, CSF ctDNA identified an established biomarker, *RET* mutation, which was undetectable in plasma ctDNA (Fig. 5B). In addition, *HGF* alteration was also detected only in BM and CSF ctDNA (Fig. 5B), which is associated with poor prognosis in cancer patients^{34,35}. In BM-LUAD 12, CSF ctDNA had a greater advantage in detecting a set of somatic alterations that occurred in BM including tumor suppressor gene mutations *TP53* and *RB1*, and investigational targets *CDK13* and *MED12* (Fig. 5C). *CDK13* regulates gene transcription and co-transcriptional processes by phosphorylating the C-terminal domain of RNA polymerase II, and its selective inhibitor shows promising effects on tumor regression³⁶. *MED12* is involved in transcription initiation and has been demonstrated to control drug responses in a variety of cancers³⁷⁻³⁹. Furthermore, patient BM-LUAD 9 developed 3 brain metastases located in the frontal lobe and cerebellum. Although MAF in plasma ctDNA here was still significantly lower than that in CSF ctDNA and BM, consistent with our data of plasma ctDNA providing equivalent efficacy to CSF ctDNA in representing profiling of multiple brain metastases (Fig. 4H), all BM mutations that were detected in both CSF ctDNA and plasma ctDNA with no significant differences (Fig. 5D). Accordingly, CSF ctDNA is a high-quality diagnostic material facilitating biomarker-based therapies for all BM, while plasma ctDNA could be an alternative liquid biopsy only in advanced NSCLC with multiple brain metastases.

Discussion

Brain metastasis is considered to diverge from primary lung cancer at an early stage. Although both sites share a “trunk” of mutations, the brain microenvironment submits the metastasis to evolve independently to harbor its own subset of unique mutations³¹. In addition, because of poor drug penetration of the blood–brain barrier, selection pressures can differ and enrich for private subclones within BM that can drive brain tumor progression divergently. Consistent with previous findings⁹, our study firstly confirmed that 61.53% of BM harbored clinically relevant mutations that were not identified in the primary tumor, with a mean of 23.65% private mutations non-detected, and many of them associated with sensitivity to targeted therapies either approved or in development such as *EGFR* and *ERBB4*^{8,40}. Brain-specific evolutionary branching strongly suggested that profiling primary tumor or extracranial metastasis is

insufficient to predict the mutational landscape of BM, and to guide targeted therapies. Considering the difficulty of brain tumor accessibility, the development and optimization of a minimally invasive biopsy to comprehensively characterize BM for assisting clinical decisions is urgent and crucial.

Advances in ctDNA sequencing and analysis largely lead to the era of precision cancer medicine, with broad applications in identifying therapeutically actionable tumor alterations, sensitive evaluation of early treatment response, dynamic monitoring of tumor recurrence and metastasis, and discovery of mechanisms of acquired resistance. Plasma ctDNA has been validated a number of times as a high-quality biomaterial of liquid biopsy in detecting and monitoring the mutations of extracranial metastasis in lung cancer. However, the absence of directly profiling the brain tumor limits the definitive comparison between BM and plasma ctDNA. To address the efficacy of plasma ctDNA in representing mutational profiles of brain metastatic sites in NSCLC, we parallelly compared the profiling of BM with plasma ctDNA, and found that more than 70% of patients harbored mutations in BM that were not detectable in plasma ctDNA. The concordance between plasma ctDNA and BM is 67.44% with a set of unidentified alterations including therapeutic biomarkers such as *EGFR*, *KRAS* and *RET*. In addition, MAF in plasma ctDNA is substantially lower than that in BM, suggesting that tumor DNA in the brain doesn't circulate well to peripheral blood or is diluted excessively. The blood-brain barrier is likely the main anatomical contributor preventing both intact tumor cells and tumor cell-free DNA from reaching the peripheral circulation system. Conversely, the BBB enriches the detection of genomic information inside CSF⁴¹. We thus explored whether CSF ctDNA is more accurate than plasma ctDNA in detecting BM mutations. Our analyses revealed that MAF in CSF ctDNA was equivalent to that in BM, and more abundant than that in plasma ctDNA, suggesting that CSF has a greater ability than plasma to detect mutations in BM, since low MAF may fall below the physical limits of ctDNA detection. MAF has been demonstrated to be associated with tumor volume²¹. We found MAF in CSF ctDNA, but not plasma ctDNA was highly correlated with the size of brain lesions, which suggests CSF ctDNA can serve as a potential predictor of molecular residual disease (MDS) and treatment response by dynamic measurement. Beyond mutational frequency analysis, our data revealed that TMB in CSF ctDNA was highly correlated with that in BM. TMB has been suggested as a potential predictive biomarker, and its dynamics during treatment can also offer prognostic information for guiding clinical management^{42,43}. Importantly, our parallel analyses indicated an average of 99.33% concordance between BM and CSF ctDNA, which demonstrated the full ability of CSF ctDNA to depict genomic mutations in BM. It is challenging to recapitulate tumor clonal diversity by analyzing a single fragment or even designed multi-region sampling due to the spatial and temporal intratumor heterogeneity⁴⁴. However, ctDNA is considered able to capture tumoral heterogeneity within or across metastatic sites. In our study, CSF ctDNA sequencing identified additional alterations to those detected in BM including *PTEN*, *DDR2* and *DNMT3A*. *PTEN* mutation is currently an inclusion criterion in 5 open clinical trials for NSCLC and one clinical trial for malignant central nervous system neoplasms. *DDR2* mutation serves as an inclusion eligibility criterion in a clinical trial targeting MGCD516, a receptor tyrosine kinase inhibitor, for patients with NSCLC, or metastatic tumors (<https://www.mycancergenome.org>). Finally, *DNMT3A* is shown to be a potential biomarker associated

with the response of immunotherapy and clinical outcome. DNMT3A is shown to be a potential biomarker associated with the response of immunotherapy and clinical outcome^{45,46}.

To further investigate the concept of CSF ctDNA in depicting mutational landscape in BM, we analyzed the matched BM, plasma ctDNA and CSF ctDNA, which demonstrated that MAF in CSF ctDNA was strongly associated with that in BM compared to plasma ctDNA. Meanwhile, TMB in CSF ctDNA, but not plasma ctDNA, was significantly correlated with that in BM. Our data further indicated that CSF ctDNA shared a significantly higher percentage of genomic alterations with BM than with plasma ctDNA. CSF ctDNA detected 51 out of 52 detectable mutations in BM, while plasma ctDNA missed 13 mutations, including several actionable mutations with targeted therapies approved or in investigation. In BM-LUAD 7, *RET* missense mutation was solely detected in CSF ctDNA. *RET* activation triggers various intracellular signaling pathways such as Ras/RAF and PI3K/AKT, which regulate cell survival, differentiation, proliferation, migration and chemotaxis⁴⁷. Selpercatinib and pralsetinib are now preferred as the first-line therapy options for patients with *RET* rearrangement–positive metastatic NSCLC according NCCN Guidelines⁸. In addition, *RET* alterations appear to be associated with a high risk of metastasis to the brain⁴⁸, and are thought to be exclusive of EGFR, ALK, KRAS and BRAF mutations, suggesting that it has its own oncogenic driver potential^{49,50}. *HGF* alteration was also detected only in CSF ctDNA. Abnormal activation of HGF could result in dysregulation of HGF/MET signaling. The FDA recently approved MET inhibitor capmatinib as a preferred targeted therapy⁸. In BM-LUAD 12, we detected common tumor suppressor genes *TP53* and *RB1*, and investigating biomarker *CDK13* and *MED12*. To date, the CDK inhibitors (CDKIs), specifically the ones that block the enzyme activity of CDK12/13 and CDK4/6, have been validated as promising therapeutic treatment in breast cancer^{36,51,52}. Accordingly, CSF ctDNA is sufficient and informative to represent the clinically relevant alterations in BM and potentially inform clinical management with superior accuracy to plasma ctDNA. Compared to brain tumor sampling, CSF ctDNA is not anticipated to be limited by sampling frequency, tumor accessibility or the existence of clinically overt disease. Of clinical interest, by associating with various features, we found that plasma ctDNA has stronger profiling performance in multiple brain metastases, equivalent to CSF ctDNA, suggesting plasma ctDNA could be an alternative liquid biopsy material to be applied in multiple brain metastatic NSCLC.

We acknowledge several limitations to our study. We performed the comparisons and analyses in a relatively small sample volume due to the challenge of BM accessibility. Validations of our findings in larger cohorts are warranted. Consistent with previous reports⁵³, the CSF ctDNA detection rate here is relatively low (11 out of 20 cases before depth filtering; factors associated with the shedding of brain tumor DNA into CSF see ref. ^{21,53}). Thus, the improvement of CSF ctDNA collection and sequencing technique would be appreciated. Additionally, our profiling of BM was obtained from accessible lesions during surgical resection in patients with multiple metastases (usually located in the same surgical region). Although spatially and temporally separated brain metastatic sites were suggested to be genetically homogenous⁹, future comprehensive profiling of all metastatic lesions would benefit further evaluation.

In conclusion, our findings demonstrate that CSF ctDNA is a high-quality diagnostic material that accurately depicts genomic profiling in BM, with greater sensitivity and specificity than plasma ctDNA, which provides CSF ctDNA a potential to guide clinical strategies of brain metastatic NSCLC management. Plasma ctDNA sequencing might still be an effective alternative for NSCLC patients with multiple brain metastases.

Methods

Study Design and Patients

Patients of newly diagnosed lung adenocarcinoma with brain metastasis were involved in this study. All 20 cases were subjected to CT scans (chest, upper abdomen including adrenal glands), MRI (brain) and bone scintigraphy. Tumor DNA was collected from surgical resections (primary lung cancer and BM) or tissue biopsy (primary lung cancer). Brain tumor removal targeted the lesion responsible for refractory intracranial pressure in multiple metastases. Five spatially distinct regions of tumor were heterogenized for tissue DNA extraction. CSF (via lumbar puncture) was obtained for ctDNA collection before brain lesion resection. The study was approved by the ethical committee in Xiangya Hospital. Written informed consents have been obtained from participants.

Histopathology And Ki67 Immunohistochemistry

Histopathological diagnosis: digital images of diagnostic tumor sections from all cases were reviewed by at least two pathologists. Ki67 immunohistochemistry analysis: immunohistochemistry was performed using anti-Ki67 (Cell Signaling Technology, #9449). The percentage of Ki67 + cells were averaged across three tumor sections for each case.

Dna Extraction And Quantification

DNA of tumor FFPE and Peripheral blood lymphocytes (PBLs) were extracted using the DNeasy Tissue and Blood Kit (Qiagen). Circulating DNA (cDNA) was isolated from plasma and cerebrospinal fluid supernatant using QIAamp Circulating Nucleic Acid Kits (Qiagen). Somatic mutations were obtained by using PBLs as the control sample to filter out germline mutations. DNA concentration was assessed using a Qubit fluorometer (Invitrogen) and the Qubit dsDNA HS Assay Kit (high sensitivity). The size distribution of circulating tumor DNA (ctDNA) was assessed using Agilent 2100 Bioanalyzer and DNA HS kit (Agilent Technologies).

Library Preparation And Sequencing

Sequencing library construction for ctDNA was performed by using the KAPA DNA Library Preparation Kit (Kapa Biosystems). Genomic DNA libraries were constructed following instruction manual of the Illumina TruSeq DNA Library Preparation Kit (Illumina). Libraries were hybridized to custom-designed biotinylated oligonucleotide probes (Roche NimbleGen) covering ~ 1.1 Mbp of 1021 genes as previously described^{54,55}. DNA sequencing was carried out with GeneSeq2000 with 100-bp paired-end reads.

Data Analysis And Somatic Mutations Calling

After collection of the sequencing data, clean reads were obtained by removing the terminal adaptor sequences and filtering out low-quality and too short sequences. Clean reads were aligned to the reference human genome (hg19) using bwa mem. Somatic single nucleotide variants (SNVs) and small insertions and deletions (InDel) were identified using MuTect and GATK software respectively by filtering out germline mutations. The candidate variants were obtained by following criteria: (i) Germline mutations with < 30% AFs in either PBL DNA or ctDNA, (ii) non-Synonymous variants with ≥ 1 reads and VAF $\geq 1\%$ in tissue. Non-Synonymous variants with ≥ 2 reads in both blood and cerebrospinal fluid²¹, (iii) Variants < 1% samples found in single nucleotide polymorphism (SNP) databases (dbSNP, <https://www.ncbi.nlm.nih.gov/projects/SNP/>; 1000G, <https://www.1000genomes.org/>; ExAC, <http://exac.broadinstitute.org/>).

Clonal Analysis

PyClone software was used to calculate cancer cell fraction (CCF) and cluster all non-synonymous somatic mutations into putative clonal clusters base on Bayesian clustering method. Somatic mutations located in the cluster with maximum CCF were defined as clonal and the rest were subclonal.

Statistical analysis

Statistical analyses and graphic visualization were performed using R (version 3.6.0.) and GraphPad Prism 8. Statistical significance was determined using Wilcoxon matched-pairs signed-rank test, Mann-Whitney *U* test (two-tailed), Friedman's test with multiple comparisons, Pearson correlation and Fisher's exact test, with $P < 0.05$ for significance for all comparisons. Data are presented as means \pm SEM.

Volumetric Analyses

Volumetric analyses of brain metastasis and peritumoral edema were determined based on enhanced T1-weighted MRI scans.

Data Availability

Data that support the findings of this study are available from the corresponding authors upon reasonable request.

Declarations

Acknowledgments

This work was supported by Swebilius Foundation (L.Z.), National Natural Science Foundation of China 81671123 (J.W).

Author contributions

L.Z and J.W. conceived and designed experiments. Surgeries were performed by J.W., Z.L., T.H., Y.W. and T.S.; data acquiring and analyzing were performed by L.Z., X.L., and M.S.; L.Z. wrote the manuscript; all authors contribute to reviewing and editing.

Conflict of interests

The authors declare no conflict of interests.

References

1. Molina, J. R., Yang, P., Cassivi, S. D., Schild, S. E. & Adjei, A. A. Non-small cell lung cancer: epidemiology, risk factors, treatment, and survivorship. *Mayo Clin Proc* **83**, 584–594, doi:10.4065/83.5.584 (2008).
2. Ulahannan, D., Khalifa, J., Faivre-Finn, C. & Lee, S. M. Emerging treatment paradigms for brain metastasis in non-small-cell lung cancer: an overview of the current landscape and challenges ahead. *Ann Oncol* **28**, 2923–2931, doi:10.1093/annonc/mdx481 (2017).
3. Leighl, N. B. *et al.* Pembrolizumab in patients with advanced non-small-cell lung cancer (KEYNOTE-001): 3-year results from an open-label, phase 1 study. *Lancet Respir Med* **7**, 347–357, doi:10.1016/S2213-2600(18)30500-9 (2019).
4. Antonia, S. J. *et al.* Four-year survival with nivolumab in patients with previously treated advanced non-small-cell lung cancer: a pooled analysis. *Lancet Oncol* **20**, 1395–1408, doi:10.1016/S1470-2045(19)30407-3 (2019).
5. Reck, M. *et al.* Updated Analysis of KEYNOTE-024: Pembrolizumab Versus Platinum-Based Chemotherapy for Advanced Non-Small-Cell Lung Cancer With PD-L1 Tumor Proportion Score of 50% or Greater. *J Clin Oncol* **37**, 537–546, doi:10.1200/JCO.18.00149 (2019).
6. Singhi, E. K., Horn, L., Sequist, L. V., Heymach, J. & Langer, C. J. Advanced Non-Small Cell Lung Cancer: Sequencing Agents in the EGFR-Mutated/ALK-Rearranged Populations. *Am Soc Clin Oncol Educ Book* **39**, e187-e197, doi:10.1200/EDBK_237821 (2019).

7. Shaw, A. T. *et al.* Crizotinib in ROS1-rearranged advanced non-small-cell lung cancer (NSCLC): updated results, including overall survival, from PROFILE 1001. *Ann Oncol* **30**, 1121–1126, doi:10.1093/annonc/mdz131 (2019).
8. Ettinger, D. S. *et al.* NCCN Guidelines Insights: Non-Small Cell Lung Cancer, Version 2.2021. *J Natl Compr Canc Netw* **19**, 254–266, doi:10.6004/jnccn.2021.0013 (2021).
9. Brastianos, P. K. *et al.* Genomic Characterization of Brain Metastases Reveals Branched Evolution and Potential Therapeutic Targets. *Cancer Discov* **5**, 1164–1177, doi:10.1158/2159-8290.CD-15-0369 (2015).
10. De Mattos-Arruda, L. *et al.* Cerebrospinal fluid-derived circulating tumour DNA better represents the genomic alterations of brain tumours than plasma. *Nat Commun* **6**, 8839, doi:10.1038/ncomms9839 (2015).
11. Paik, P. K. *et al.* Next-Generation Sequencing of Stage IV Squamous Cell Lung Cancers Reveals an Association of PI3K Aberrations and Evidence of Clonal Heterogeneity in Patients with Brain Metastases. *Cancer Discov* **5**, 610–621, doi:10.1158/2159-8290.CD-14-1129 (2015).
12. Cescon, D. W., Bratman, S. V., Chan, S. M. & Siu, L. L. Circulating tumor DNA and liquid biopsy in oncology. *Nature Cancer* **1**, 276–290, doi:10.1038/s43018-020-0043-5 (2020).
13. Alix-Panabieres, C. & Pantel, K. Liquid Biopsy: From Discovery to Clinical Application. *Cancer Discov* **11**, 858–873, doi:10.1158/2159-8290.CD-20-1311 (2021).
14. Moding, E. J., Nabet, B. Y., Alizadeh, A. A. & Diehn, M. Detecting Liquid Remnants of Solid Tumors: Circulating Tumor DNA Minimal Residual Disease. *Cancer Discov*, doi:10.1158/2159-8290.CD-21-0634 (2021).
15. Stadler, J. C. *et al.* Current and future clinical applications of ctDNA in immuno-oncology. *Cancer Res*, doi:10.1158/0008-5472.CAN-21-1718 (2021).
16. Heitzer, E., Haque, I. S., Roberts, C. E. S. & Speicher, M. R. Current and future perspectives of liquid biopsies in genomics-driven oncology. *Nat Rev Genet* **20**, 71–88, doi:10.1038/s41576-018-0071-5 (2019).
17. Chaudhuri, A. A. *et al.* Early Detection of Molecular Residual Disease in Localized Lung Cancer by Circulating Tumor DNA Profiling. *Cancer Discov* **7**, 1394–1403, doi:10.1158/2159-8290.CD-17-0716 (2017).
18. Pantel, K. & Alix-Panabieres, C. Liquid biopsy and minimal residual disease - latest advances and implications for cure. *Nat Rev Clin Oncol* **16**, 409–424, doi:10.1038/s41571-019-0187-3 (2019).
19. Cabel, L. *et al.* Clinical potential of circulating tumour DNA in patients receiving anticancer immunotherapy. *Nat Rev Clin Oncol* **15**, 639–650, doi:10.1038/s41571-018-0074-3 (2018).
20. Moding, E. J. *et al.* Circulating Tumor DNA Dynamics Predict Benefit from Consolidation Immunotherapy in Locally Advanced Non-Small Cell Lung Cancer. *Nat Cancer* **1**, 176–183, doi:10.1038/s43018-019-0011-0 (2020).
21. Abbosh, C. *et al.* Phylogenetic ctDNA analysis depicts early-stage lung cancer evolution. *Nature* **545**, 446–451, doi:10.1038/nature22364 (2017).

22. Chabon, J. J. *et al.* Integrating genomic features for non-invasive early lung cancer detection. *Nature* **580**, 245–251, doi:10.1038/s41586-020-2140-0 (2020).
23. Coakley, M., Garcia-Murillas, I. & Turner, N. C. Molecular Residual Disease and Adjuvant Trial Design in Solid Tumors. *Clin Cancer Res* **25**, 6026–6034, doi:10.1158/1078-0432.CCR-19-0152 (2019).
24. Li, B. T. *et al.* Ultra-deep next-generation sequencing of plasma cell-free DNA in patients with advanced lung cancers: results from the Actionable Genome Consortium. *Ann Oncol* **30**, 597–603, doi:10.1093/annonc/mdz046 (2019).
25. Aggarwal, C. *et al.* Clinical Implications of Plasma-Based Genotyping With the Delivery of Personalized Therapy in Metastatic Non-Small Cell Lung Cancer. *JAMA Oncol* **5**, 173–180, doi:10.1001/jamaoncol.2018.4305 (2019).
26. Clark, T. A. *et al.* Analytical Validation of a Hybrid Capture-Based Next-Generation Sequencing Clinical Assay for Genomic Profiling of Cell-Free Circulating Tumor DNA. *J Mol Diagn* **20**, 686–702, doi:10.1016/j.jmoldx.2018.05.004 (2018).
27. Nabavizadeh, S. A. *et al.* Imaging and histopathologic correlates of plasma cell-free DNA concentration and circulating tumor DNA in adult patients with newly diagnosed glioblastoma. *Neurooncol Adv* **2**, vdaa016, doi:10.1093/noajnl/vdaa016 (2020).
28. Pentsova, E. I. *et al.* Evaluating Cancer of the Central Nervous System Through Next-Generation Sequencing of Cerebrospinal Fluid. *J Clin Oncol* **34**, 2404–2415, doi:10.1200/JCO.2016.66.6487 (2016).
29. Li, Y. S. *et al.* Unique genetic profiles from cerebrospinal fluid cell-free DNA in leptomeningeal metastases of EGFR-mutant non-small-cell lung cancer: a new medium of liquid biopsy. *Ann Oncol* **29**, 945–952, doi:10.1093/annonc/mdy009 (2018).
30. Wang, Y. *et al.* Unique genomic alterations of cerebrospinal fluid cell-free DNA are critical for targeted therapy of non-small cell lung cancer with leptomeningeal metastasis. *Genomics*, doi:10.1016/j.ygeno.2021.11.015 (2021).
31. Stricker, T. & Arteaga, C. L. Drug-Resistant Brain Metastases: A Role for Pharmacology, Tumor Evolution, and Too-Late Therapy. *Cancer Discov* **5**, 1124–1126, doi:10.1158/2159-8290.CD-15-1166 (2015).
32. Shen, Z. *et al.* INPP4B mutation as a novel biomarker for immunotherapy in patients with non-small cell lung cancer. *Cancer Research* **80**, 4287 (Suppl):Abstract (2020).
33. Bettgowda, C. *et al.* Detection of circulating tumor DNA in early- and late-stage human malignancies. *Sci Transl Med* **6**, 224ra224, doi:10.1126/scitranslmed.3007094 (2014).
34. Ma, J. *et al.* Somatic mutation and functional polymorphism of a novel regulatory element in the HGF gene promoter causes its aberrant expression in human breast cancer. *J Clin Invest* **119**, 478–491, doi:10.1172/JCI36640 (2009).
35. Huang, X. *et al.* Targeting the HGF/MET Axis in Cancer Therapy: Challenges in Resistance and Opportunities for Improvement. *Front Cell Dev Biol* **8**, 152, doi:10.3389/fcell.2020.00152 (2020).

36. Quereda, V. *et al.* Therapeutic Targeting of CDK12/CDK13 in Triple-Negative Breast Cancer. *Cancer Cell* **36**, 545–558 e547, doi:10.1016/j.ccell.2019.09.004 (2019).
37. Huang, S. *et al.* MED12 controls the response to multiple cancer drugs through regulation of TGF-beta receptor signaling. *Cell* **151**, 937–950, doi:10.1016/j.cell.2012.10.035 (2012).
38. Rosell, R. Mediating resistance in oncogene-driven cancers. *N Engl J Med* **368**, 1551–1552, doi:10.1056/NEJMcibr1214549 (2013).
39. Rosell, R., Bivona, T. G. & Karachaliou, N. Genetics and biomarkers in personalisation of lung cancer treatment. *Lancet* **382**, 720–731, doi:10.1016/S0140-6736(13)61715-8 (2013).
40. Rauf, F. *et al.* Ibrutinib inhibition of ERBB4 reduces cell growth in a WNT5A-dependent manner. *Oncogene* **37**, 2237–2250, doi:10.1038/s41388-017-0079-x (2018).
41. Ghersi-Egea, J. F. *et al.* Molecular anatomy and functions of the choroidal blood-cerebrospinal fluid barrier in health and disease. *Acta Neuropathol* **135**, 337–361, doi:10.1007/s00401-018-1807-1 (2018).
42. Gandara, D. R. *et al.* Blood-based tumor mutational burden as a predictor of clinical benefit in non-small-cell lung cancer patients treated with atezolizumab. *Nat Med* **24**, 1441–1448, doi:10.1038/s41591-018-0134-3 (2018).
43. Wang, Z. *et al.* Assessment of Blood Tumor Mutational Burden as a Potential Biomarker for Immunotherapy in Patients With Non-Small Cell Lung Cancer With Use of a Next-Generation Sequencing Cancer Gene Panel. *JAMA Oncol* **5**, 696–702, doi:10.1001/jamaoncol.2018.7098 (2019).
44. de Bruin, E. C. *et al.* Spatial and temporal diversity in genomic instability processes defines lung cancer evolution. *Science* **346**, 251–256, doi:10.1126/science.1253462 (2014).
45. Husni, R. E. *et al.* DNMT3a expression pattern and its prognostic value in lung adenocarcinoma. *Lung Cancer* **97**, 59–65, doi:10.1016/j.lungcan.2016.04.018 (2016).
46. Zhang, L. *et al.* Small extracellular vesicles control dendritic spine development through regulation of HDAC2 signaling. *J Neurosci*, doi:10.1523/JNEUROSCI.0766-20.2021 (2021).
47. Arighi, E., Borrello, M. G. & Sariola, H. RET tyrosine kinase signaling in development and cancer. *Cytokine Growth Factor Rev* **16**, 441–467, doi:10.1016/j.cytogfr.2005.05.010 (2005).
48. Drilon, A. *et al.* Frequency of Brain Metastases and Multikinase Inhibitor Outcomes in Patients With RET-Rearranged Lung Cancers. *J Thorac Oncol* **13**, 1595–1601, doi:10.1016/j.jtho.2018.07.004 (2018).
49. Takeuchi, K. *et al.* RET, ROS1 and ALK fusions in lung cancer. *Nat Med* **18**, 378–381, doi:10.1038/nm.2658 (2012).
50. Drusbosky, L. M., Rodriguez, E., Dawar, R. & Ikpeazu, C. V. Therapeutic strategies in RET gene rearranged non-small cell lung cancer. *J Hematol Oncol* **14**, 50, doi:10.1186/s13045-021-01063-9 (2021).
51. Zhang, M. *et al.* CDK inhibitors in cancer therapy, an overview of recent development. *Am J Cancer Res* **11**, 1913–1935 (2021).

52. Tadesse, S., Duckett, D. R. & Monastyrskiy, A. The promise and current status of CDK12/13 inhibition for the treatment of cancer. *Future Med Chem* **13**, 117–141, doi:10.4155/fmc-2020-0240 (2021).
53. Miller, A. M. *et al.* Tracking tumour evolution in glioma through liquid biopsies of cerebrospinal fluid. *Nature* **565**, 654–658, doi:10.1038/s41586-019-0882-3 (2019).
54. Chen, Y. *et al.* Association of Tumor Protein p53 and Ataxia-Telangiectasia Mutated Comutation With Response to Immune Checkpoint Inhibitors and Mortality in Patients With Non-Small Cell Lung Cancer. *JAMA Netw Open* **2**, e1911895, doi:10.1001/jamanetworkopen.2019.11895 (2019).
55. Shi, J. *et al.* Genomic Landscape and Tumor Mutational Burden Determination of Circulating Tumor DNA in Over 5,000 Chinese Patients with Lung Cancer. *Clin Cancer Res* **27**, 6184–6196, doi:10.1158/1078-0432.CCR-21-1537 (2021).

Figures

Fig. 1

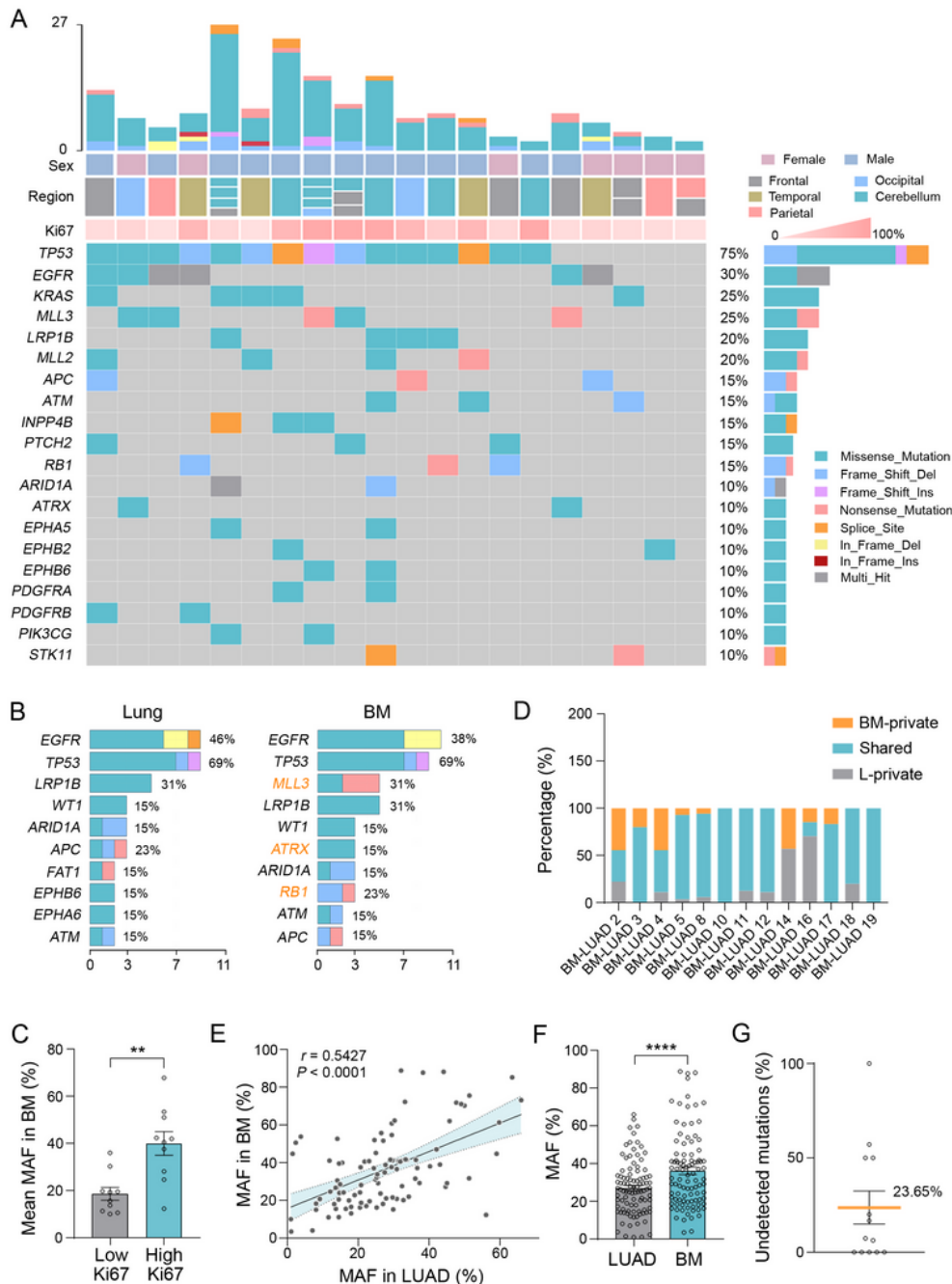


Figure 1

Somatic mutations in primary lung adenocarcinoma and brain metastasis. **A:** Mutational landscape of brain metastases (BM). Tumor mutational burden (TMB) is shown in the top bar graph. Top heat maps indicate key patient characteristics including sex, metastatic region and number, and Ki67 index. Bottom heat maps present mutational landscape of top 20 alterations. Mutational rate is depicted in the right bar graph. **B:** Beyond high frequency mutations shared with the primary tumor, BM has unique frequent

mutations in *MLL3*, *ATRX* and *RB1*. **C:** Quantification shows the mean mutant allele fraction (MAF) in BM is significantly higher in lesions with high Ki67 ($\geq 30\%$) expression (Mann-Whitney test, **: $P \leq 0.01$). **D:** Stacked bar graphs depict BM-private, shared and lung adenocarcinoma (L)-private mutations in each individual patient. **E:** MAF in BM is correlated with that in primary lung cancer (each circle represents a shared mutation in both BM and primary lung cancer; Pearson $r = 0.5427$, $P \leq 0.0001$). **F:** Bar graph of MAF in primary lung cancer and BM (Wilcoxon signed-rank test, ****: $P \leq 0.0001$). **G:** Bar graph indicates 23.65% (95% CI, 0%-50%) mutations in BM were undetectable in primary lung cancer. Data are presented as means+SEM.

Fig. 2

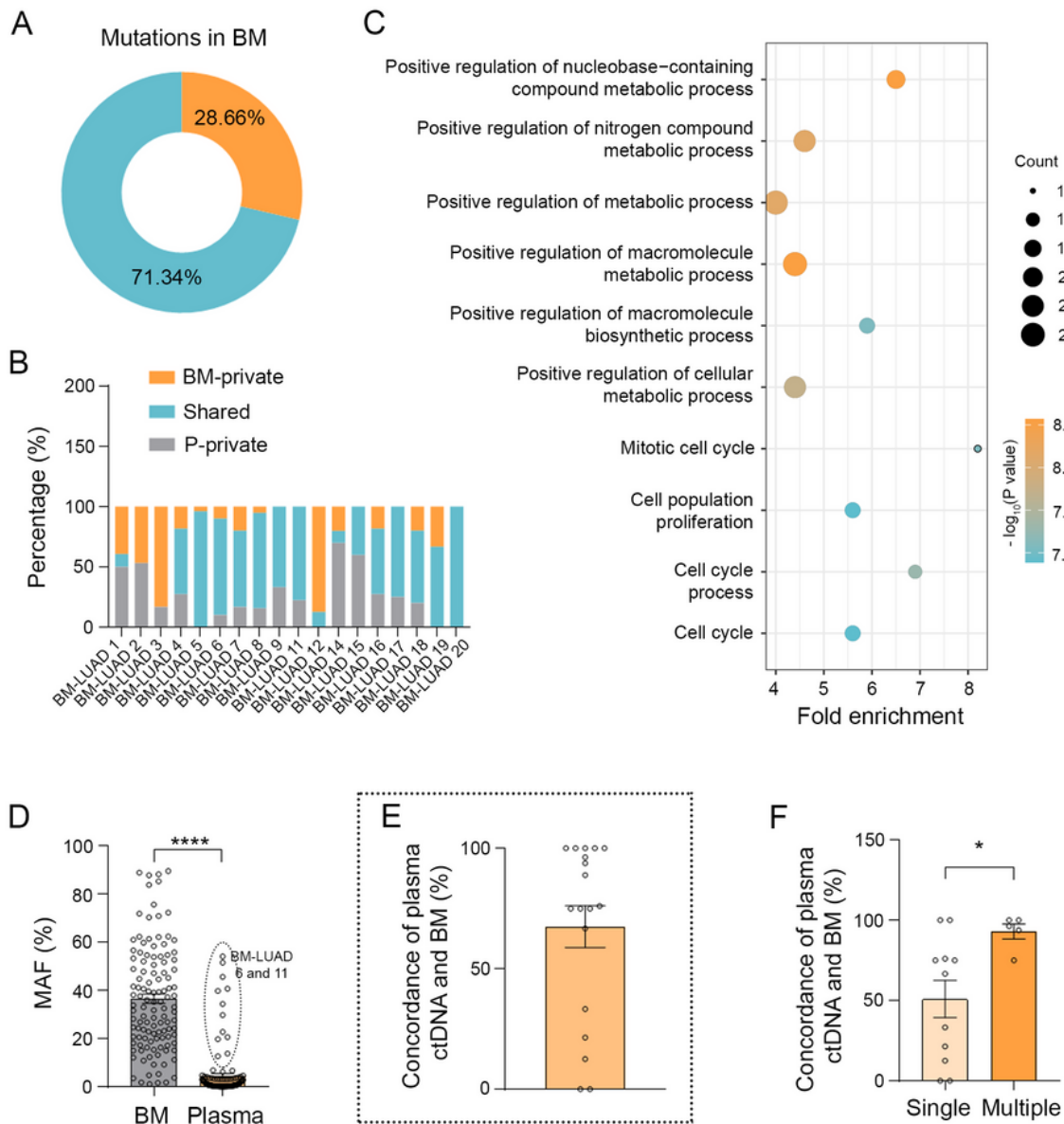


Figure 2

Plasma ctDNA is not sufficient to inclusively describe BM mutations. **A:** Pie chart shows the percentage of detected (28.66%) and undetected mutations of BM using plasma ctDNA sequencing. **B:** Stacked bar graphs depict BM-private, shared and plasma ctDNA (P)-private mutations in each individual patient. **C:** Pathway analysis indicates the undetected genomic alterations are enriched mainly in metabolic and cell cycle related processes. **D:** Bar graph of MAF of matched mutations in plasma ctDNA and BM. BM-LUAD

6 and 11 developed extracranial metastases in liver and thyroid, respectively (Wilcoxon signed-rank test, ****: $P \leq 0.0001$). **E:** Bar graph shows the mean concordance (67.44%) between BM and plasma ctDNA. **F:** Quantification indicates that plasma ctDNA has significantly higher concordance with BM in patients with multiple metastases (Mann-Whitney test, *: $P \leq 0.05$). Data are presented as means+SEM.

Fig. 3

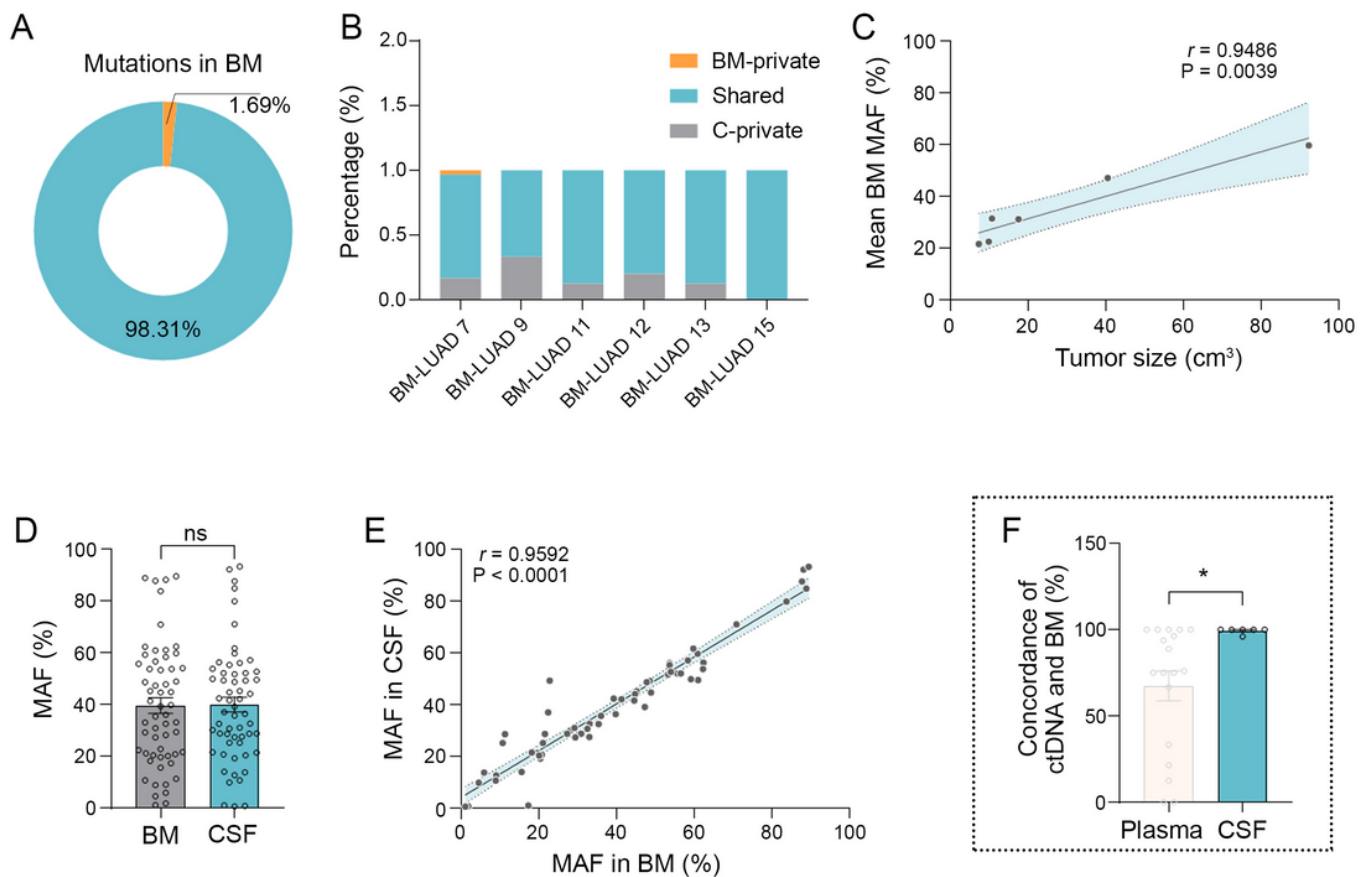


Figure 3

CSF ctDNA recapitulates the mutations in single BM. **A:** Pie chart indicates that 98.31% mutations in BM are detectable in CSF ctDNA. **B:** Stacked bar graphs depict BM-private, shared and CSF ctDNA-private mutations in each individual patient. **C:** Plots show MAF in CSF ctDNA is associated with the size of brain lesion (Pearson $r = 0.9486$, $P = 0.0039$). **D-E:** Quantification shows MAF in CSF ctDNA is equivalent and highly associated with that in BM (D: Wilcoxon signed-rank test, ns: not significant; E: Pearson $r = 0.9486$, $P = 0.0039$). **F:** Bar graph of concordance between BM and CSF ctDNA or plasma ctDNA (99.33% vs.

67.44%, concordance data of plasma ctDNA is from Fig. 2E; Mann-Whitney test, *: $P \leq 0.05$). Data are presented as means+SEM.

Fig. 4

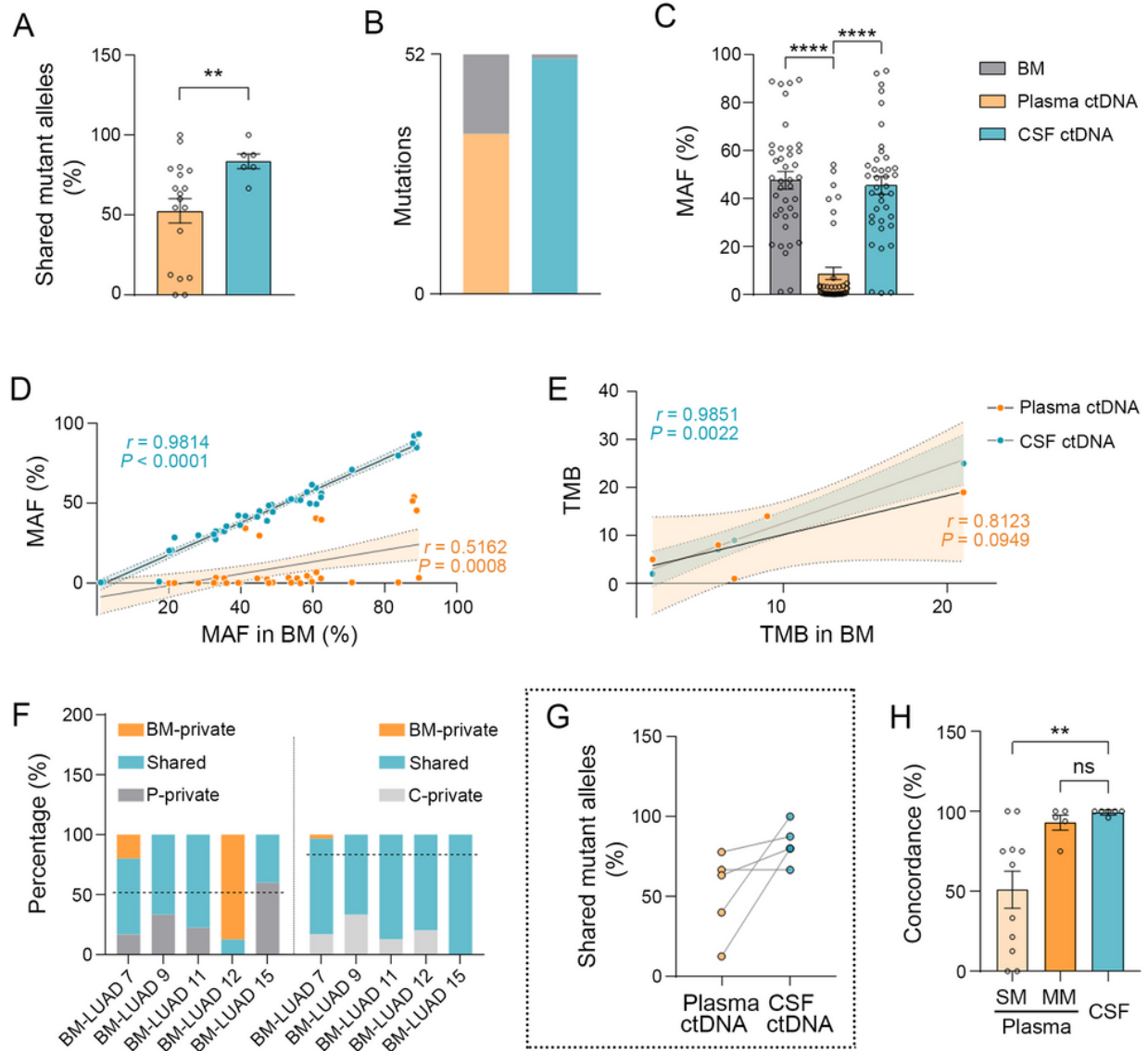


Figure 4

CSF ctDNA is better than plasma ctDNA in presenting mutations in single BM. **A:** Bar graph of the percentage of shared mutant alleles between BM and plasma ctDNA or CSF ctDNA (percentage was

calculated by dividing the number of shared mutations to the total number of mutations detected by sequencing in BM and CSF ctDNA or plasma ctDNA, each circle represents a single patient; Mann-Whitney test, **: $P \leq 0.01$). **B:** Bar graph shows CSF ctDNA detected 51 out of 52 alterations in BM, while only 39 alterations were detected in plasma ctDNA (Fisher exact test, $P = 0.0009$). **C:** Bar graphs of MAF in matched BM, plasma ctDNA and CSF ctDNA (Friedman test, ****: $P \leq 0.0001$). **D:** MAF in CSF ctDNA is more strongly correlated with that in BM compared to plasma ctDNA (CSF ctDNA: Pearson $r = 0.9814$, $P \leq 0.0001$; plasma ctDNA: Pearson $r = 0.5162$, $P = 0.0008$). **E:** Plots shows TMB in BM has a stronger correlation with that in CSF ctDNA than plasma ctDNA (CSF ctDNA: Pearson $r = 0.9851$, $P = 0.0022$; plasma ctDNA: Pearson $r = 0.8123$, $P = 0.0949$). **F:** Stacked bar graphs present BM-private, shared and CSF (C) ctDNA-private or plasma ctDNA (P)-private mutations in each individual. **G:** Percentage quantification of shared mutations (with matched plasma ctDNA or CSF ctDNA) in BM (Wilcoxon signed-rank test, $P = 0.0625$). **H:** Bar graphs show that CSF ctDNA and plasma ctDNA have similar concordance with BM in patients with multiple metastases, and significantly higher than that of single metastasis (SM: single metastasis, MM: multiple metastases, Mann-Whitney test, **: $P \leq 0.01$, ns: not significant). Data are presented as means+SEM.

Fig. 5

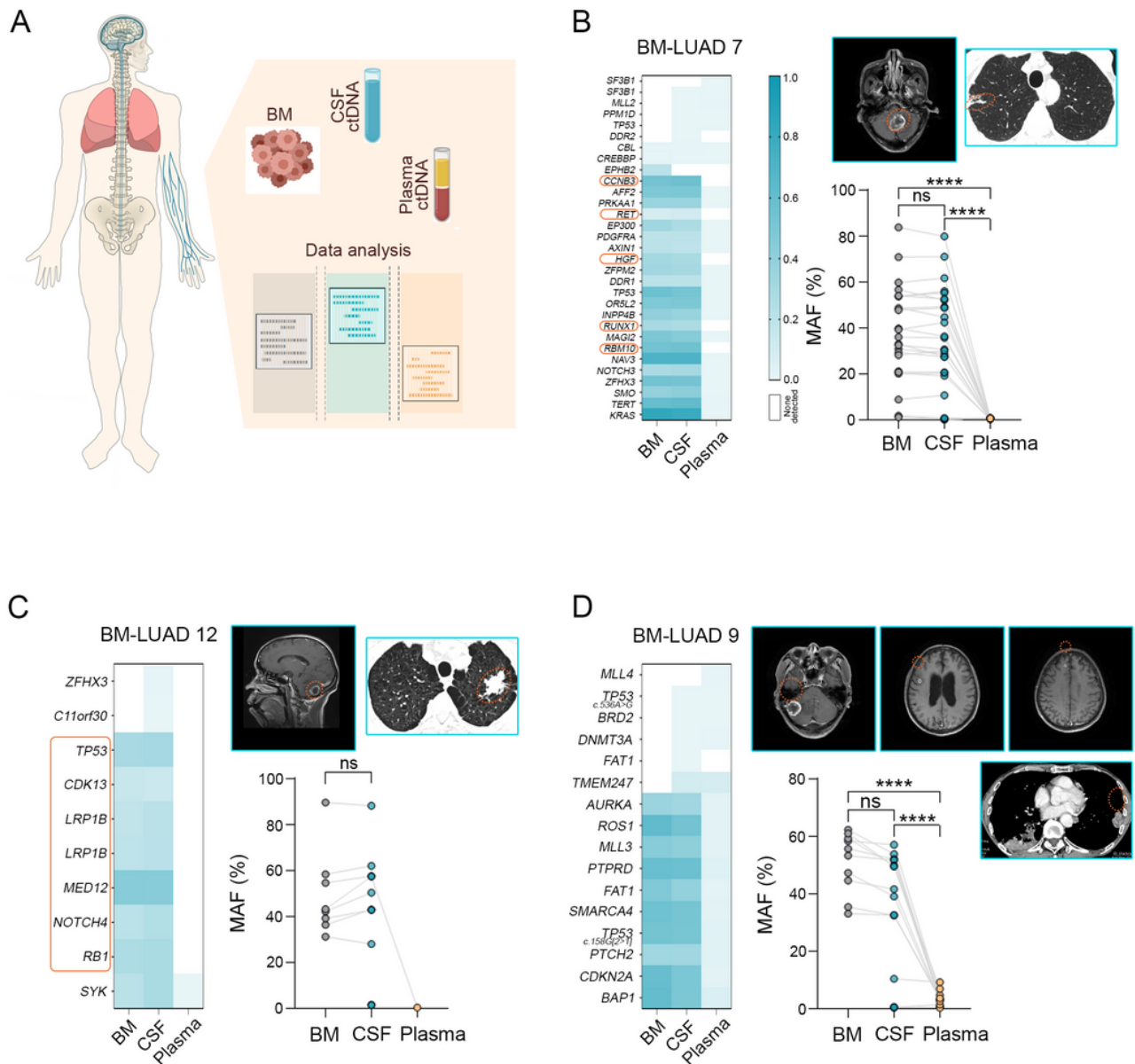


Figure 5

CSF ctDNA provides potential molecular targets in advanced lung cancer patients with BM. **A:** Diagram of the experimental procedures. **B:** Patient BM-LUAD 7 detected several mutations solely in BM and CSF ctDNA, including actionable somatic mutation *RET*. Left: heat maps of detected genomic alterations in BM, CSF ctDNA and plasma ctDNA; right top: radiographic information (brain: MRI, lung: CT); right bottom: MAF in each sample (Mann-Whitney test, ****: $P < 0.0001$, ns: not significant). **C:** Patient BM-LUAD 12 has mutations in tumor suppressor genes *TP53* and *RB1*, and investigational target genes *CDK13* and *MED12*

that were only identified in BM and CSF ctDNA, but not in plasma ctDNA (ns: not significant). **D:** BM-LUAD 9 confirms that plasma ctDNA is an optional liquid biopsy in the condition of multiple brain metastases in advanced NSCLC (Mann-Whitney test, ****: $P \leq 0.0001$, ns: not significant).

Supplementary Files

This is a list of supplementary files associated with this preprint. Click to download.

- [SupplementaryMaterial.pdf](#)